Possible Synergistic Effect of Platelet Rich Plasma and Losartan on Experimentally Induced Skeletal Muscle Injury in Adult Male Albino Rats: A Histological and an Immunohistochemical Study

Original Article

Amira Hashem Mohamed Neanaa, Moushira Aly Reda El-Heneidy, Hoda Mahmoud Ahmed Khalifa and Silvia Kamil Seddik Sawires

Department of Histology and Cell Biology, Faculty of Medicine, University of Alexandria, Egypt

ABSTRACT

Introduction: Minimization of the disability after skeletal muscle injuries is still a challenge. Understanding of the contribution of growth factors has sparked a lot of interest in platelet-rich plasma therapy (PRP). Another line of treatment is the usage of anti-fibrotic agents as losartan.

Aim of the Work: Was to test the therapeutic effect of PRP, losartan and their combined treatment on skeletal muscle injury.

Materials and Methods: Forty two adult male albino rats were distributed into 2 groups: Group I (Control uninjured group) and Group II (Treated injured rats' group). The latter was further subdivided into 4 equal subgroups and received: no treatment, single intramuscular injection of 100 μL PRP, single dose of 10 mg/kg/day losartan by oral gavage, and combined treatment of PRP and losartan respectively. The rats were sacrificed and light and electron microscopy were performed to examine the specimens of gastrocnemius muscle. In addition, immunohistochemical staining for CD 34 was performed.

Results: Subgroup IIA showed interrupted muscle fibers with focal areas of myofibrillar loss. Meanwhile, subgroups IIB and IIC revealed more regenerative changes. Evident hypercellularity with variable migrating cells were detected. In addition, neovascularization in some areas of subgroup IIC was noticed. Subgroup IID showed renewed muscle fibers in different stages with few structural changes. The results of the immuno-stained samples showed a positive reaction along the boundaries of some muscle fibers in subgroup IIA. Whereas the positive reaction in IIB, IIC and IID subgroups extended to the lateral borders and within some affected fibers and around the new pale nuclei, expressing advanced muscle regeneration.

Conclusions: After a muscle contusion, a combination of PRP and losartan treatment may enhance overall skeletal muscle recovery.

INTRODUCTION

The most prevalent sports-related injuries are skeletal muscle injuries, which provide a problem for primary care and sports medicine. Athletes experience muscle injuries from a variety of sources, including direct damage (e.g. strains, lacerations, and contusions) and indirect injuries (related to ischemia and neurological dysfunctions)[1]. Among which, muscle contusions are the most frequently encountered in athletes and military personnel. Due to the reduced range of motion and pain caused by such injuries, muscle's capacity to function and perform can be hampered[2].

Current conservative therapies for skeletal muscle injuries include controlling bleeding with elevation and compression, local cooling, non-steroidal anti-inflammatory medications (NSAIDs) and physical therapy are used to improve full functional recovery and reduce impairment[3]. Increased awareness of the role of growth factors in the repair of wounded tissue has sparked a surge in interest in the use of platelet-rich plasma (PRP) over the last decade[4].

Platelet-rich plasma (PRP) is an autologous blood-derived product that becomes attractive therapeutic option in regenerative medicine for its powerful healing properties. Its regenerative capacity is attributed to at least fifteen different factors that are known to be contained within platelets, including platelet derived growth factor (PDGF), transforming growth factor-β (TGF-β), vascular endothelial growth factor (VEGF), epidermal growth factor (EGF), and insulin growth factor (IGF)[5,6].

Compared to synthetic biomaterials, PRP augments regenerative processes or physiologic healing without interfering with their homeostatic balance, the cost for its preparation is less expensive and can be prepared on-site in a timely manner so it is suitable for smaller or office-based clinics[7]. In addition, being autologous diminishes the hazards of rejection or immune response and it has an antimicrobial effect as it contains leukocytes, resulting in

lower risk of infection[8]. TGF-β1, a growth factor present in high amounts in PRP, could increase fibrosis in injured skeletal muscle. After a muscular injury, an increase in fibrosis enhances the chance of re-injury[9]. The dominant role of TGF-β1 in skeletal muscle fibrosis makes it a clear objective for several anti-fibrotic agents that disable TGF-β1 signaling cascade[10]. Among these antifibrotic agents, losartan is the first orally active commercially available antihypertensive angiotensin II type 1 receptor blocker used to treat hypertension and congestive heart failure. It indirectly blocks TGF-β1 signaling cascade and enhances the physiological function of injured muscle[11,12].

Losartan has been found to improve muscle regeneration, diminish the fibrotic region and improve muscle function in models of contusion and laceration[13]. When administered on the third or seventh day following an injury or trauma, it has a beneficial effect[14]. Based on these facts, the goal of this research was to study the histological changes in an experimental model of mechanical skeletal muscle injury and to appraise the ameliorating effect of platelet rich plasma, losartan and their combined treatment on the healing of the skeletal muscle after the contusion injury.

MATERIALS AND METHODS

Animals

Forty two male albino rats aged 12 weeks with an average weight 250 g were purchased from and raised at the Animal House of the Physiology Department, Faculty of Medicine, Alexandria University. Standard housing conditions of temperature, humidity and 12 hours light/dark cycle, were applied. Further, they were allowed unrestricted access to laboratory food and water. All the experimental trials followed the code of research ethics approved by the Research Ethics Committee, Alexandria Faculty of Medicine.

Experimental design

The animals were divided into two groups at random as following:

Group I (Control group): 18 rats, which were subdivided into 3 equal subgroups; subgroup IA: 6 uninjured rats, subgroup IB: 6 uninjured rats received a single intramuscular injection of distilled water (100 μL) and subgroup IC: 6 uninjured rats served as a donor for PRP.

Group II: 24 injured rats, which were subdivided into 4 equal subgroups; subgroup IIA (untreated subgroup): 6 rats received no treatment, subgroup IIB (PRP subgroup): 6 rats received a single intramuscular injection of a PRP solution (100 μL) within 2 hours after injury at the site of the muscle lesion[15], subgroup IIC (losartan subgroup): 6 rats were given commercially accessible losartan (AMRIYA PHARM, IND.) dissolved in the water they consume by oral gavage at the dosage level of 10 mg/kg body weight /day, from day 3 from the time of injury through the end of the experiment after 3 weeks[16] and subgroup IID

(PRP+ losartan subgroup): 6 rats received combined treatment of PRP and losartan as the same dose and duration of subgroups IIB and IIC.

Blood collection and preparation of platelet rich plasma

The PRP preparation was conducted at the Clinical Pathology Lab, Alexandria Faculty of Medicine. Fresh blood was drawn from all rats via retro-orbital venous plexus after being anesthetized by ether inhalation into a sterile syringe containing 1ml of 3.8% sodium citrate. For preparation of PRP, the blood was centrifuged twice after being placed into blood tubes containing the anticoagulant citrate phosphate dextrose. The first centrifugation was done at 1000 rpm for 15 minutes at 4°C. The supernatant obtained was aspirated by micropipette, and then placed in another sterile tube. A second cycle of centrifugation at 1000 rpm for 15 minutes at 4°C was done where platelets were aggregated in the bottom of the tube in the form of pellet[17]. Only about 1 ml of the heavier centrifuged material remained after the supernatant portion was removed. The platelet concentration, or PRP, was the name given to this fraction. Using a pipette approach, the platelet-rich fraction of the supernatant was separated and maintained at room temperature.

The concentration of platelets in the PRP was measured using an automated cell counter to guarantee that the concentration was at least 4 times the whole blood levels. PRP activation was done by adding 0.1ml of calcium chloride to each 1ml of PRP and was injected at the site of injury by using an insulin syringe within 10 minutes of activation[15].

Induction of muscle injury

Under anesthesia, each animal was placed prone in the injury device with the hind limb fully extended. This confirmed a direct impact on the gastrocnemius muscle's mid-belly region. A mass weighing 350 g was dropped from a height of 50 cm over the mid belly region of the gastrocnemius muscles, causing the injury[15]. The device used for producing the experimental injuries was designed and manufactured at the Production Department, Faculty of Engineering, Alexandria University. (Figures 1a, 1b).

Fig.1a: A photo illustrating muscle contusion device.
Fig. 1b: A photo illustrating the production of the muscle contusion injury.

Histological study

At the end of the experiment (3 weeks from the day of injury), all rats were sacrificed under anesthesia. The gastrocnemius muscles of each animal were dissected and the middle part of each muscle was excised and cut into 2 specimens; one for the light microscopic examination and the other for electron microscopic study.

1. Light microscopy: specimens were fixed in 10% formol saline, dehydrated in ascending grades of alcohol, cleared in xylol and embedded in paraffin to prepare paraffin blocks. 5 µ thick transverse and longitudinal sections were prepared and stained with hematoxylin and eosin. H&E[18], Masson's trichrome[19] and immunohistochemical stain with anti-CD34,[20] one of the satellite cells surface markers.

2. Transmission electron microscopy: muscle specimens were obtained, cut into 1mm3, fixed in 3% phosphate-buffered glutaraldehyde at pH 7.4 at 4 oC and then processed to get ultrathin stained sections[21]. Electron micrographs were obtained by using TEM (JEM-1400 Plus, Japan) equipped with a digital camera at Electron Microscopy Unit, Faculty of Science, Alexandria University.

Immuno-histochemical study

Routine immuno-histochemical avidin–biotin method was used for detection of CD34 positive satellite cells in the muscle (which is one of the satellite cells surface markers) at the Clinical Pathology Department, Faculty of Medicine, Alexandria University.

The paraffin sections were deparaffinized in xylol, rehydrated in graded alcohol series and embedded in 3% H_2O_2 in methanol to inhibit endogenous peroxidase. For epitope retrieval, the sections were rinsed in distilled water and heated in a microwave oven (in citrate buffer 10 mM, pH6) for 15 minutes. The slides were incubated first with normal horse serum (1/30 avidin 10%) for CD34 and then in biotin for 10 min. A Vector Blocking kit (Vector Laboratories; Burlingame, CA) was used to hinder endogenous biotin then the slides were incubated at 20 oC for 40 min with monoclonal antibodies for CD34. The slides were incubated with anti-mouse/rabbit biotinylated bridging antibodies (dilution 1/200) for 30 min then the sections were washed and incubated with standard avidin–biotin complex (ABC; Dako Cytomation, Glostrup, Denmark) for 30 min. H2O2 was used as a substrate and diaminobenzidine was used as a chromogen to demonstrate antibody binding followed by hematoxylin counterstain[20]. Then the slides were examined by a light microscope.

Morphometric study and statistical analysis

Collagen % area quantification

From Masson's trichrome-stained sections of each subgroup, with a 10X objective lens magnification, 6 random fields were manually picked and imaged. Image

J software (version 1.51k, Wayne Rasband, National Institutes of Health, USA) was utilized for the analysis. Colored images were analyzed by the color threshold tool and the pixels were measured with the measure tool. Data were analyzed using IBM SPSS software package version 20.0 (Armonk, NY: IBM Corp). Quantitative data were defined using range, mean, standard deviation and median. *P-values* ≤0.05 were considered statistically significant.

RESULTS

Histological results

Light microscopic results

Hematoxylin and eosin stain

Control group (Group I): Light microscopic examination of longitudinal sections of the rat gastrocnemius muscles of the control subgroups (IA, IB) revealed the normal appearance of skeletal muscle fibers. The muscle fibers were cylindrical in shape and parallel to each other with eosinophilic sarcoplasm and multiple flattened nuclei which were peripherally situated beneath the sarcolemma (Figures 2 a,b).

Group II:

Subgroup IIA (untreated subgroup): Examination of the gastrocnemius muscles of this subgroup revealed obvious structural changes, where most of the skeletal muscle fibers appeared injured and interrupted (Figures 3 a,d). Pale stained nuclei were seen migrating towards the injured fibers (Figure 3b). Congestion of the blood vessels and extravasation of the blood were further observed in some areas (Figures 3 a,b). Moreover, massive cellular proliferation was depicted forming a multinucleated syncytium (Figure 3c). The injured fibers were associated in some areas with deposition of fibrous tissue (Figure 3d).

Subgroup IIB (PRP subgroup): The gastrocnemius muscles of rats of this subgroup revealed injured and interrupted muscle fibers (Figures 4 a,b). Besides, some fibers showed deeply situated lightly stained oval nuclei, while fibrous tissue deposition in wide injured areas was also noticed. Many adipocytes filling the narrow injured areas and interfibrillar migrating variable cells were further encountered (Figure 4a). Massive cellular proliferation forming multinucleated syncytium was also detected at the site of injury (Figure 4b).

Subgroup IIC (Losartan subgroup): On examination of sections of the gastrocnemius muscles of this subgroup, some muscle fibers appeared injured and interrupted, while others revealed splitting and branching with deeply situated lightly stained nuclei. Evident cellular migration towards the defected sites was found as well as neovascularization in other areas. Limited collagen fibers deposition at the large defective areas was also recognized (Figures 5 a,b).

Subgroup IID (Losartan+PRP subgroup): Examination of the gastrocnemius muscles of this subgroup revealed regenerating fibers at different stages with few structural

changes, where most of the muscle fibers appeared pale eosinophilic with multiple deeply situated and sub-sarcolemmal lightly stained nuclei forming myotubes. Some fibers appeared splitted and branched with dark peripheral nuclei (Figure 6). Cross bridging of some fibers with pale eosinophilic sarcoplasm and dark peripheral nuclei with other fibers with darker sarcoplasm and deeply situated pale nuclei were also noticed (Figure 7).

Masson's trichrome stain

Examination of Masson's trichrome sections of subgroups IIA and IIB revealed increased deposition of collagen fibers in between the injured fibers, in the endomysium, in the perimysium and the perivascular area as compared to the control subgroups (IA and IB). While examination of the gastrocnemius muscles of subgroup IIC exhibited a relatively small amount of collagen fibers in the same areas. On the other hand, in subgroup IID almost the control pattern of collagen distribution was observed (Figures 8 a-f).

Immunohistochemical results

Immunohistochemically stained sections for CD34 expression in the rat gastrocnemius muscles of the control group (IA and IB) depicted negative reaction in the sarcoplasm and nuclei of the skeletal muscle fibers (Figure 9a). The untreated subgroup IIA showed positive reaction along the boundaries of some muscle fibers, in the connective tissue, within the proliferating cells and around the blood vessels in between the muscle fibers (Figure 9b). Subgroup IIB revealed positive reaction at the periphery and inside the injured muscle fibers as well as in the connective tissue (Figure 9c), while subgroup IIC showed limited positive reaction around the new pale nuclei inside the injured fibers and along its sarcolemma (Figure 9d). The positive reaction in subgroup IID was observed inside some injured muscle fibers and surrounding the nuclei that aligned at the sarcolemma of some others (Figure 9e).

Electron microscopic results

Control group (Group I)

Electron microscopic examination of the ultra-thin sections of the gastrocnemius muscle of the control subgroups (IA and IB) showed skeletal muscle fibers invested by the sarcolemma with sub-sarcolemmal elongated nuclei. The fibers were mainly formed by myofibrils with alternating dark and light bands that occurred in register resulting in striated pattern of the muscle fibers. The dark band (A-band) was bisected by a paler H-band, which itself was bisected by a dense M-line. The light band (I-band) was bisected by a dense line called Z-line. Mitochondria were seen at the poles of the nuclei and in the spaces between the myofibrils (Figures 10 a,b).

Group II

Subgroup IIA (untreated subgroup): Ultrastructural examination of the gastrocnemius muscle of this subgroup revealed many striated muscle fibers with focal areas of myofibrillar loss (Figures 11 a,b). Multiple nuclei were detected in some muscle fibers either sub-sarcolemmal (Figure 11a) or deeply situated with irregular outline (Figure 11c). Depositions of collagen fibers and irregular blood vessels as well as colloid like material were also noticed at the site of injury (Figures11 b,c). Few fibers showed accumulation of lysosomes at the perinuclear area (Figure 11d). Aggregation of numerous pleomorphic mitochondria at the site of myofibrillar loss with irregular arrangement was further encountered (Figures 11 a,b,c). Longitudinally oriented matted giant mitochondria were seen in between the myofibrils, some of which were transversely oriented as well (Figures 12 a,b). Disrupted mitochondrial cristae and rupture of its membranes were occasionally detected (Figures 11 d,b). In addition, some fibers revealed prominent T-tubules at the site of myofibrillar loss (Figure 12b)

Subgroup IIB (PRP subgroup): Ultrastructural examination of the gastrocnemius muscle of this subgroup showed some striated muscle fibers with areas of interrupted myofibrils (Figure 13a). Irregularly arranged and disarrayed myofibrils in some fibers were also noticed (Figure 13b). Several migratory cells were depicted either in between the myofibers (Figures 14 a,b) or aligned along their borders with cytoplasmic processes bordering the neighboring cells (Figure 15).

Irregular euchromatic nuclei either sub-sarcolemmal (Figure 13b) or deeply situated (Figure 15) were also detected in some fibers of this subgroup. Moreover, aggregates of proliferating pleomorphic mitochondria either at the edges of some injured muscle fibers (Figure 13a) or sub-sarcolemmal (Figure 13b) were seen. Additionally, collagen fibers deposits and blood vessels (Figure 13a) as well as colloid like material (Figures 13 a,b) at the site of injury were also found.

Subgroup IIC (Losartan subgroup): Examination of the gastrocnemius muscle of rats of this subgroup showed some interrupted muscle fibers (Figure 16a) and multiple focal areas of myofibrillar loss (Figures 16 b,,c) with disrupted striations (Figure 16c). Euchromatic irregular nuclei were also detected either sub-sarcolemmal (Figure 16b) or migratory towards some injured areas (Figure16a). Accumulation of numerous pleomorphic mitochondria at the sites of myofibrillar loss (Figures 16 a,b) was noticed, some were transversely oriented (Figure 16c). Moreover, migratory blood vessels occupying the site of injury of some muscle fibers were depicted surrounded by numerous mitochondria (Figure 16a). Some interrupted myofibers were surrounded by small ovoid migratory cells. Blood vessels and colloidal-like material were seen surrounding the migratory cells as well (Figure 16d).

Subgroup IID (Losartan+PRP subgroup): Ultrastructural examination of the gastrocnemius muscle of this subgroup showed striated muscle fibers

with limited areas of injured and interrupted myofibrils (Figures 17 a,b), some retrieval of its continuity (Figure 17b). Nearly all muscle fibers were well registered (Figures 17 a-d) with few focal areas of myofibrillar loss (Figures 17 a,c,d). Sub-sarcolemmal euchromatic nuclei (Figure17c) and few mitochondria at the site of myofibrillar loss were detected (Figs. 17 a-c), some were large and matted together (Figure 17c), others were transversely oriented (Figure 17d). Evident T-tubules (Figure 17d) were depicted in some fibers as well. Migratory blood vessels (Figure 17a) and colloidal-like material (Figures 17 a,b) were also noticed at the site of injury of some fibers.

Morphometric results

The mean area percentage of collagen did not exhibit any significant difference between the different control subgroups (IA and IB) ($P > 0.05$). It was significantly increased in subgroups IIA, IIB and IIC as compared to the control subgroups, whereas subgroup IID did not show any significant difference with respect to the control subgroups. On comparing the different subgroups of group II, the mean area % of collagen was significantly higher in subgroup IIA with respect to other subgroups (IIB, IIC, IID). Meanwhile, significantly lower value was depicted in subgroup IID as compared to subgroups IIB and IIC.
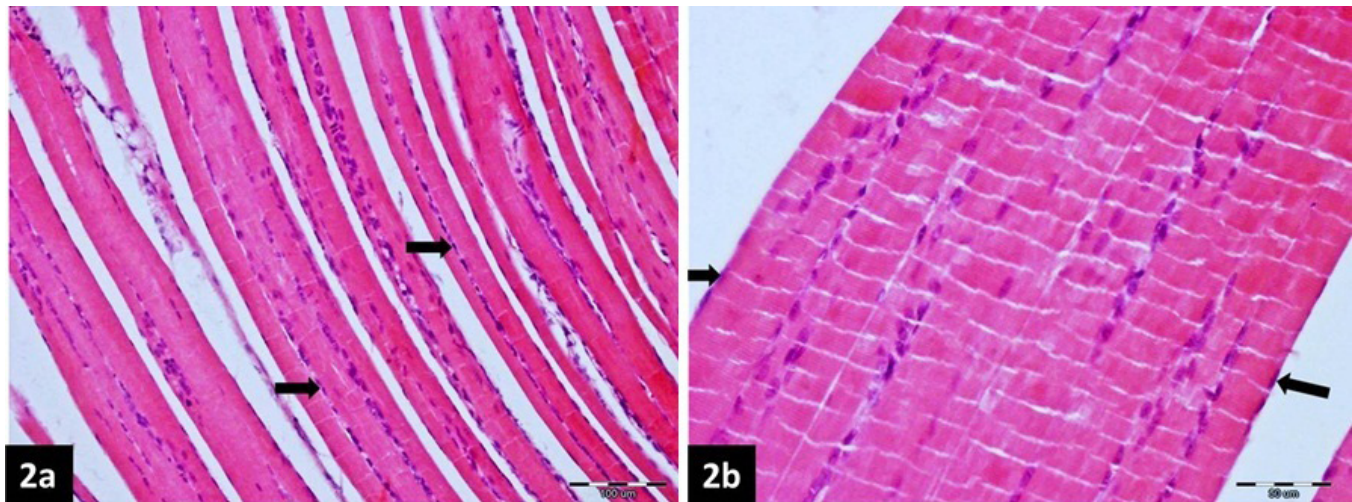
Figs. 2a, b: Light photomicrographs of longitudinal sections of gastrocnemius muscle of the control subgroups (IA and IB) showing parallel cylindrical muscle fibers with an eosinophilic sarcoplasm and multiple peripheral flattened nuclei (arrows). Mic. Mag. 2a) X200 , 2b) X400
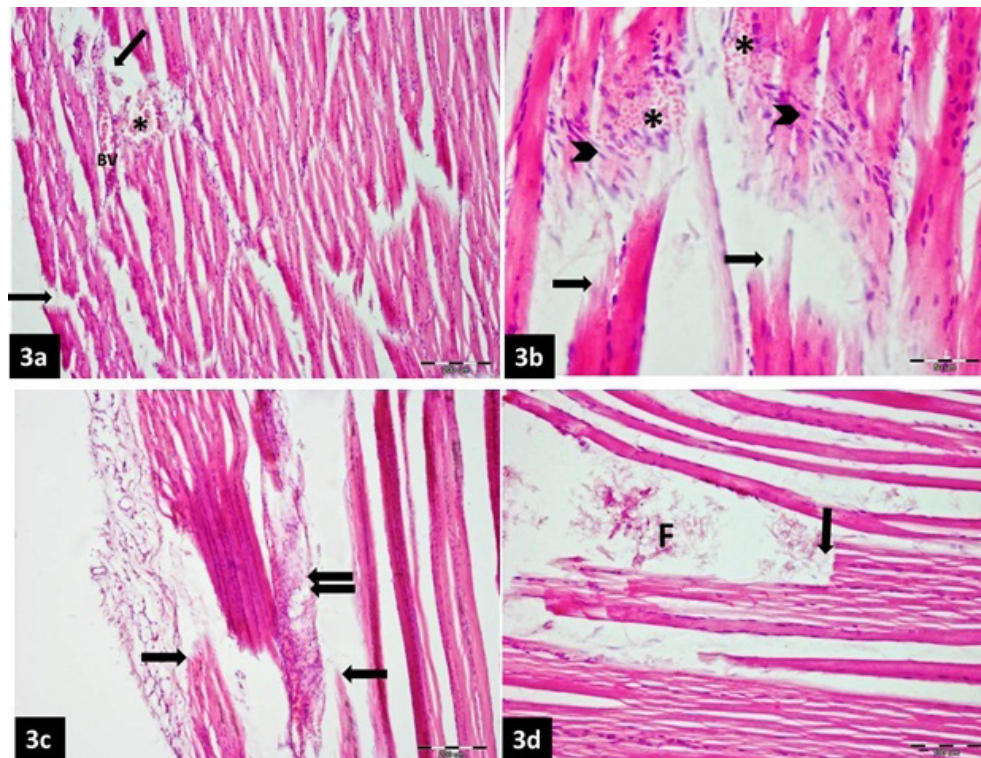
Figs. 3 a-d: Light photomicrographs of longitudinal sections of a rat gastrocnemius muscle of the subgroup IIA (untreated group) revealing injured and interrupted muscle fibers (arrows). 3a- injured area showing congested blood vessel (BV) and extravasation of blood (*). 3b- Some areas showing waves of migrating cells towards the site of injury (arrowheads) and an extravasation of blood (*). 3c- Massive cellular proliferation forming multinucleated syncytium (double arrow). d- Deposition of fibrous tissue (F) is seen at the site of injury. Mic. Mag. 3a& 3c) X100, 3b) X400, 3d) X200.
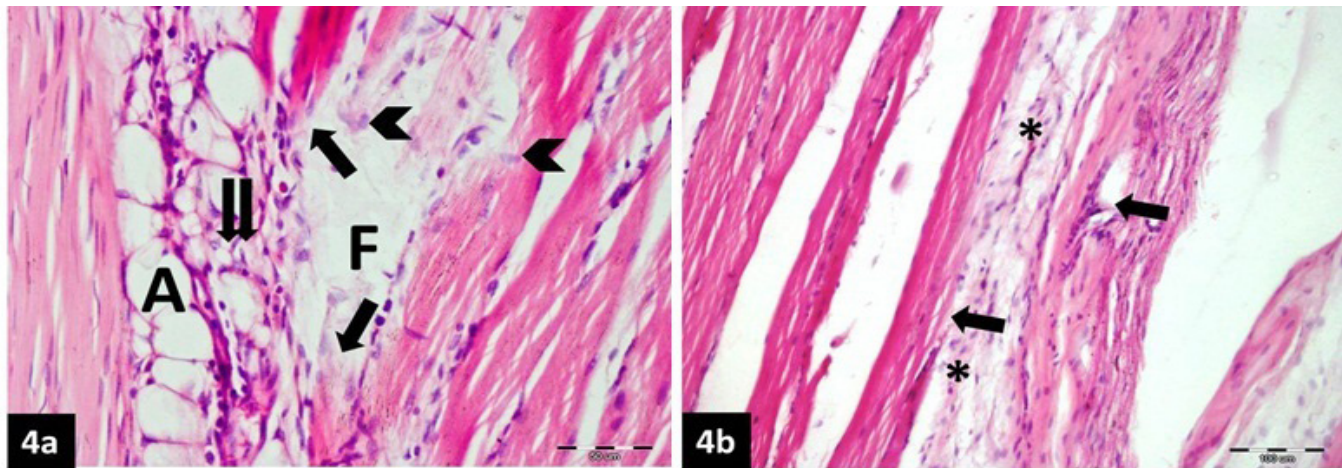
Figs. 4 a, b: Light photomicrographs of longitudinal sections of a rat gastrocnemius muscle of subgroup IIB (PRP subgroup) revealing injured and interrupted muscle fibers (arrows). 4a- Some fibers show deeply situated lightly stained oval nuclei (arrowheads). Many adipocytes (A) closing the narrow injured area and interfibrillar migrating cells (double arrow) are also seen. F; fibrous tissue. 4b- The site of injury revealing massive cellular proliferation forming multinucleated syncytium (*). Mic. Mag. 4a) X400, 4b) X200
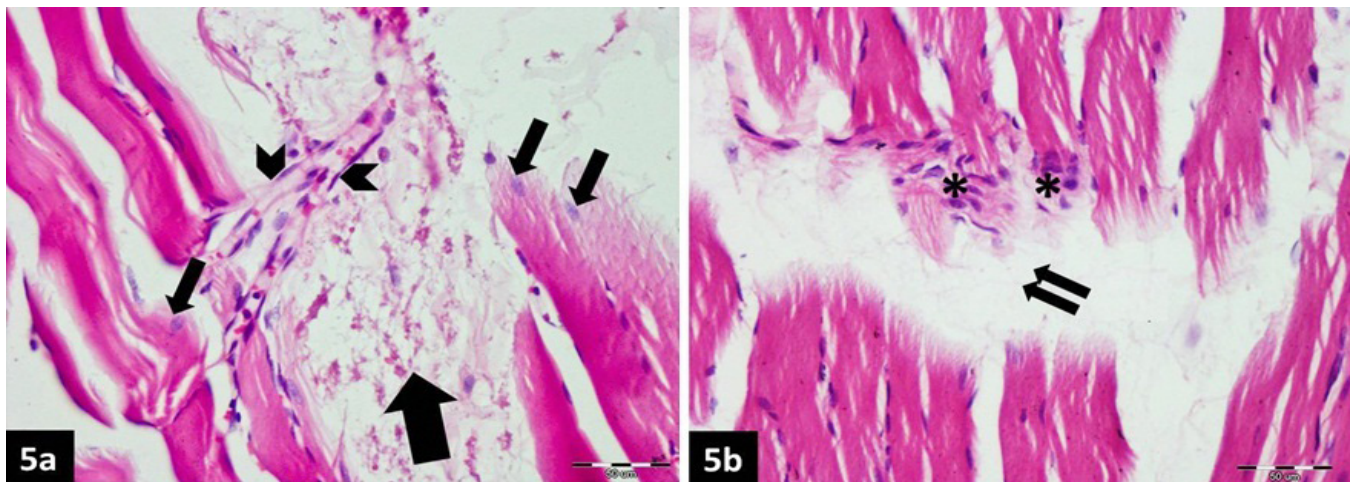
Figs. 5 a, b: Light photomicrographs of longitudinal sections of a rat gastrocnemius muscle of the subgroup IIC (losartan subgroup) showing some injured and interrupted muscle fibers. 5a- Rows of cells and blood vessels (arrowheads) are extending towards the defective sites. Other muscle fibers show splitting and branching along its length and reveal deeply situated lightly stained nuclei (arrows). Notice: the extravasated RBCs with some fibrous tissue at the defective large areas (thick arrow). 5b- An evident cellular migration of many oval pale stained nuclei towards the edges of injured fibers (*). Notice the limited collagen deposition in the large interfibrillar gap (double arrow). Mic. Mag. X400
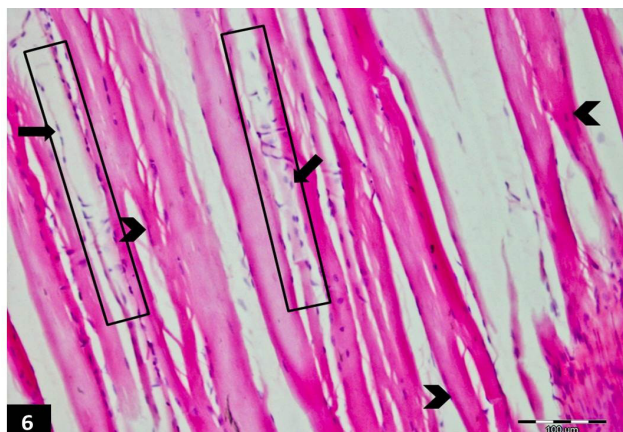
Fig. 6: A light photomicrograph of a longitudinal section of a rat gastrocnemius muscle of the subgroup IID (PRP+ losartan subgroup) showing regenerating muscle fibers, some reveal pale eosinophilic sarcoplasm with multiple lightly stained nuclei (arrows) aligned along the sarcolemma and others are deeply situated forming long tubal structure (rectangle). Other fibers show splitting and branching along their length with dark stained peripheral nuclei (arrowheads). Mic. Mag. X 200.
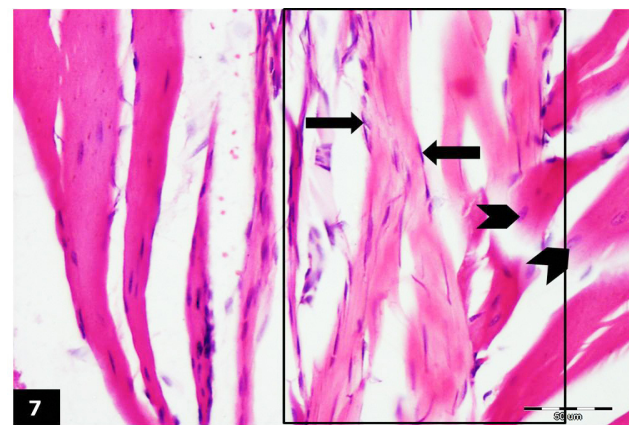
Fig. 7: A light photomicrograph of longitudinal section of subgroup IID revealing some interrupted muscle fibers that cross bridge with each other (rectangle), some of them reveal pale eosinophilic sarcoplasm with dark peripheral nuclei (arrows), others show darker sarcoplasm with pale deeply situated nuclei (arrowheads). Mic. Mag. X 400
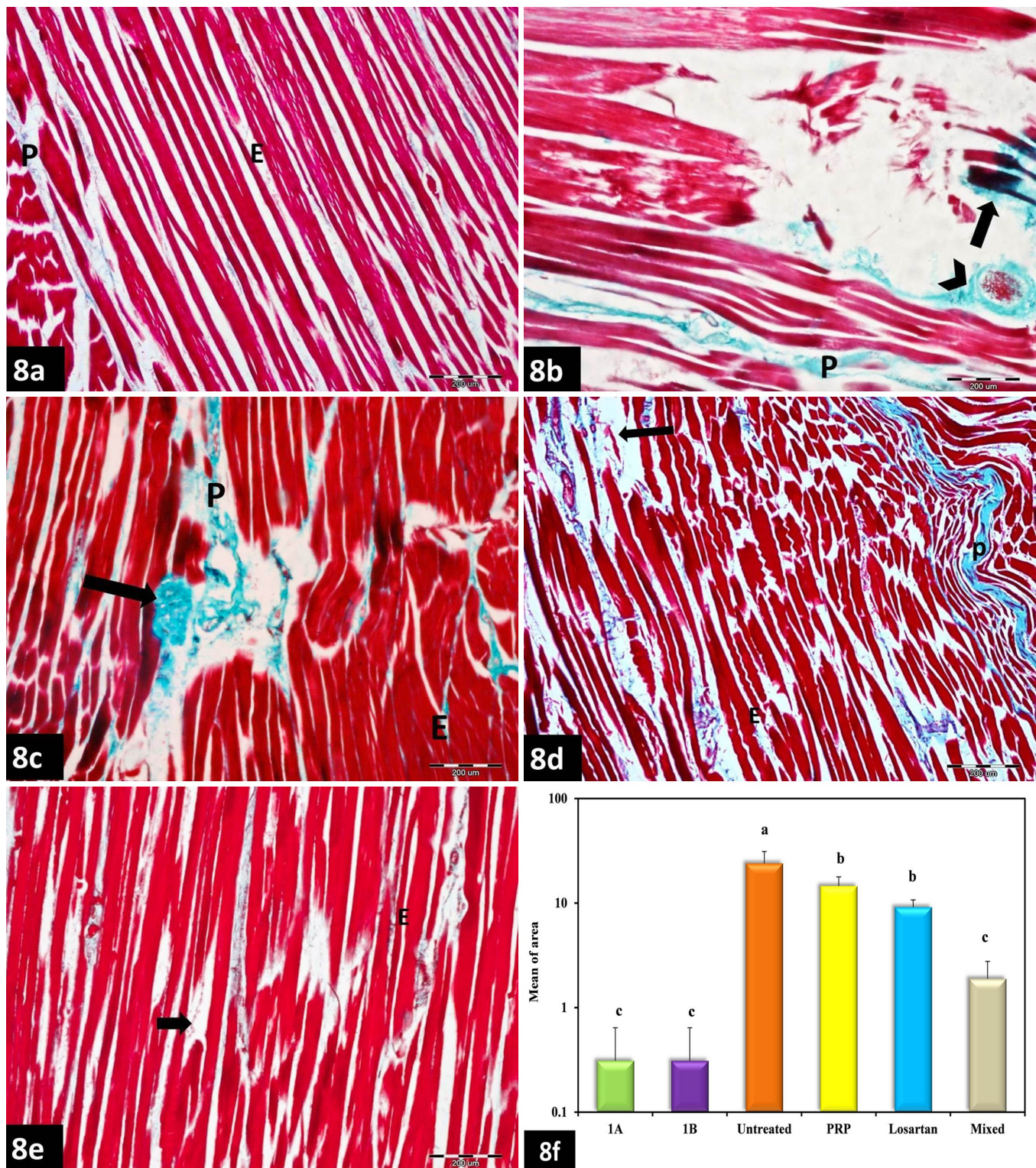
Figs. 8 a-e: Photomicrographs of longitudinal sections of a rat gastrocnemius muscle of the different subgroups stained by Masson's trichrome showing different degrees of collagen deposition. 8a- Control subgroup IA showing scanty amount of collagen fibers in the endomysium (E). It is slightly increased in the perimysium (P). 8b- Subgroup IIA (untreated subgroup) revealing excessive deposition of collagen fibers at the area of damaged fibers (arrow). Thick bundles of collagen fibers are also seen in the perimysium (P) and surrounding the blood vessels (arrowhead). 8c- Subgroup IIB (PRP subgroup) with thick collagen bundles at the area of injured fibers (arrow), in the endomysium (E) and in the perimysium (P). 8d- Subgroup IIC (losartan subgroup) showing scanty amount of collagen fibers in the endomysium (E) and at the damaged area (arrow) and more in the perimysium (P). 8e- Subgroup IID (PRP+ losartan subgroup) showing a minimal amount of collagen fibers in between the injured muscle fibers (arrow) and in the endomysium (E). Mic. Mag. X100 .

Fig. 8 f: A histogram showing comparison between the studied groups according to the area percentage of the collagen. Values represent mean ± SD. Statistical significance was determined using ANOVA and Post Hoc (Tukey). Different letters are statistically significant at $p \leq 0.05$.
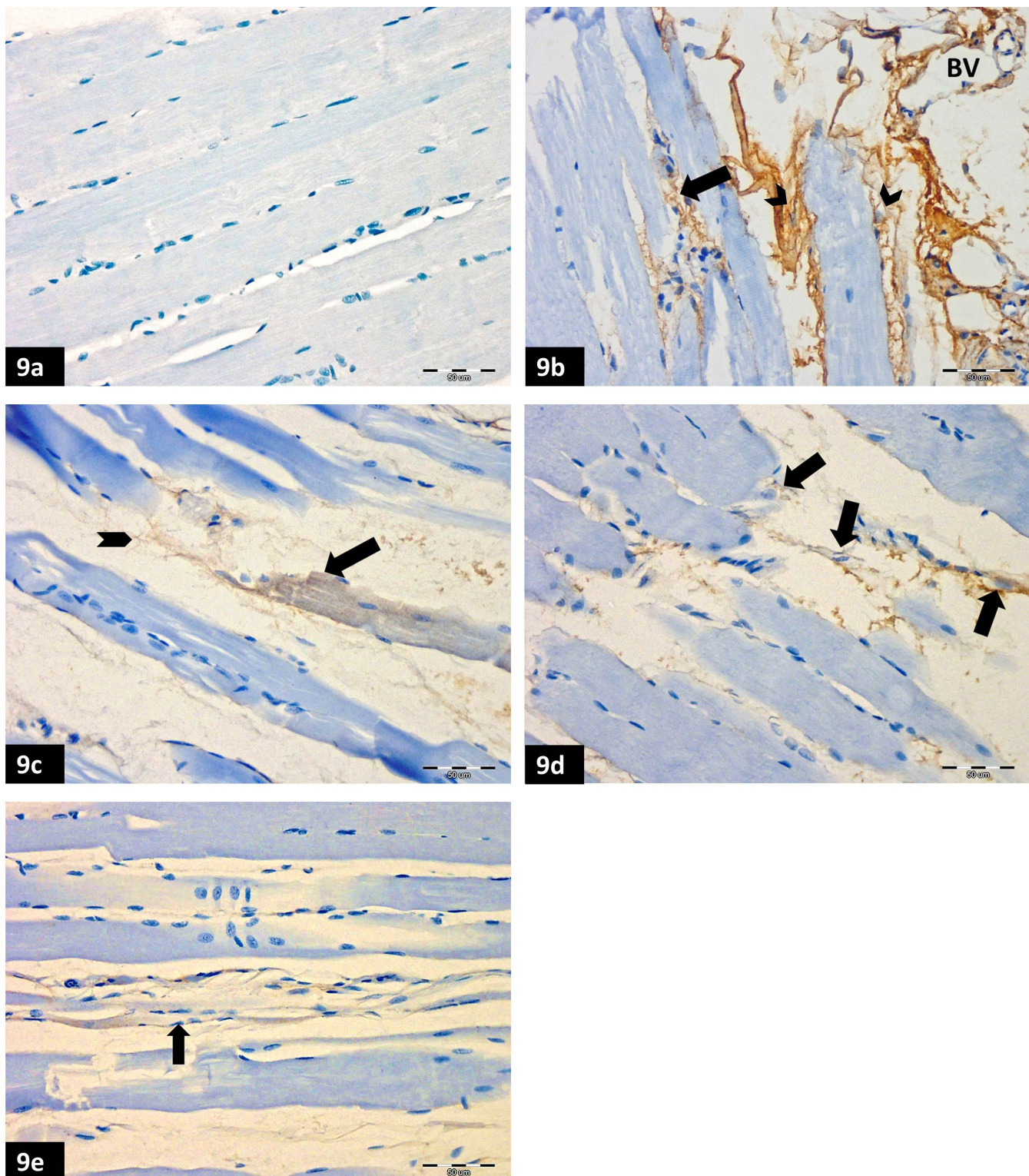
Figs. 9 a-e: Photomicrographs of longitudinal sections of a rat gastrocnemius muscle of the different subgroups for immunohistochemical evaluation of CD34 expression. 9a- Control subgroup IA showing negative reaction in the sarcoplasm of the muscle fibers. 9b- Subgroup IIA (untreated subgroup) showing strong positive immunoreaction along the boundaries of injured fibers (arrowheads), within proliferating cells (arrow), in the connective tissue and around the blood vessels (BV) in between the injured muscle fibers. 9c- Subgroup IIB (PRP subgroup) illustrating positive immunoreaction at the periphery and inside injured muscle fibers (arrow). Another reaction is seen in the connective tissue (arrowhead). 9d- Subgroup IIC (losartan subgroup) showing positive immunoreaction limited around the new pale nuclei (arrows) which appear inside the injured fibers and along its sarcolemma. 9e- Subgroup IID (PRP+ losartan subgroup) showing positive immunoreaction surrounding the nuclei that aligned along the sarcolemma of an injured muscle fiber (the newly formed myoblast tube) (arrow). Mic. Mag. X400.
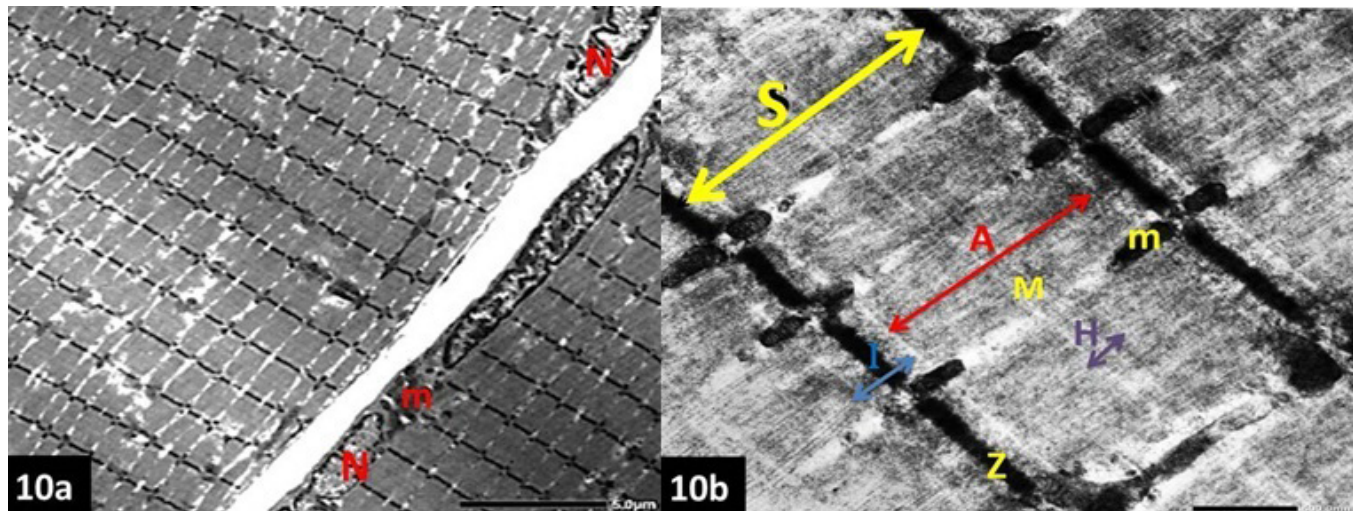
Figs. 10a, b: Electron micrographs of a gastrocnemius muscle of control subgroups (IA and IB). 10a- Showing striated muscle fibers with elongated sub-sarcolemmal heterochromatic nuclei (N) and perinuclear mitochondria (m). The sarcoplasm is filled with bundles of myofibrils showing alternating dark and light bands that occur in register. 10b- The myofibrils showing alternating dark bands (A) bisected by the H-zone (H) and M-line (M), and the light bands (I) bisected by the Z-lines (Z). The length of sarcomeres (S) of different myofibrils is nearly equal. Longitudinally oriented mitochondria (m) are noticed at the intermyofibrillar spaces. Mic. Mag. 10a) X1500, 10b) X10000.
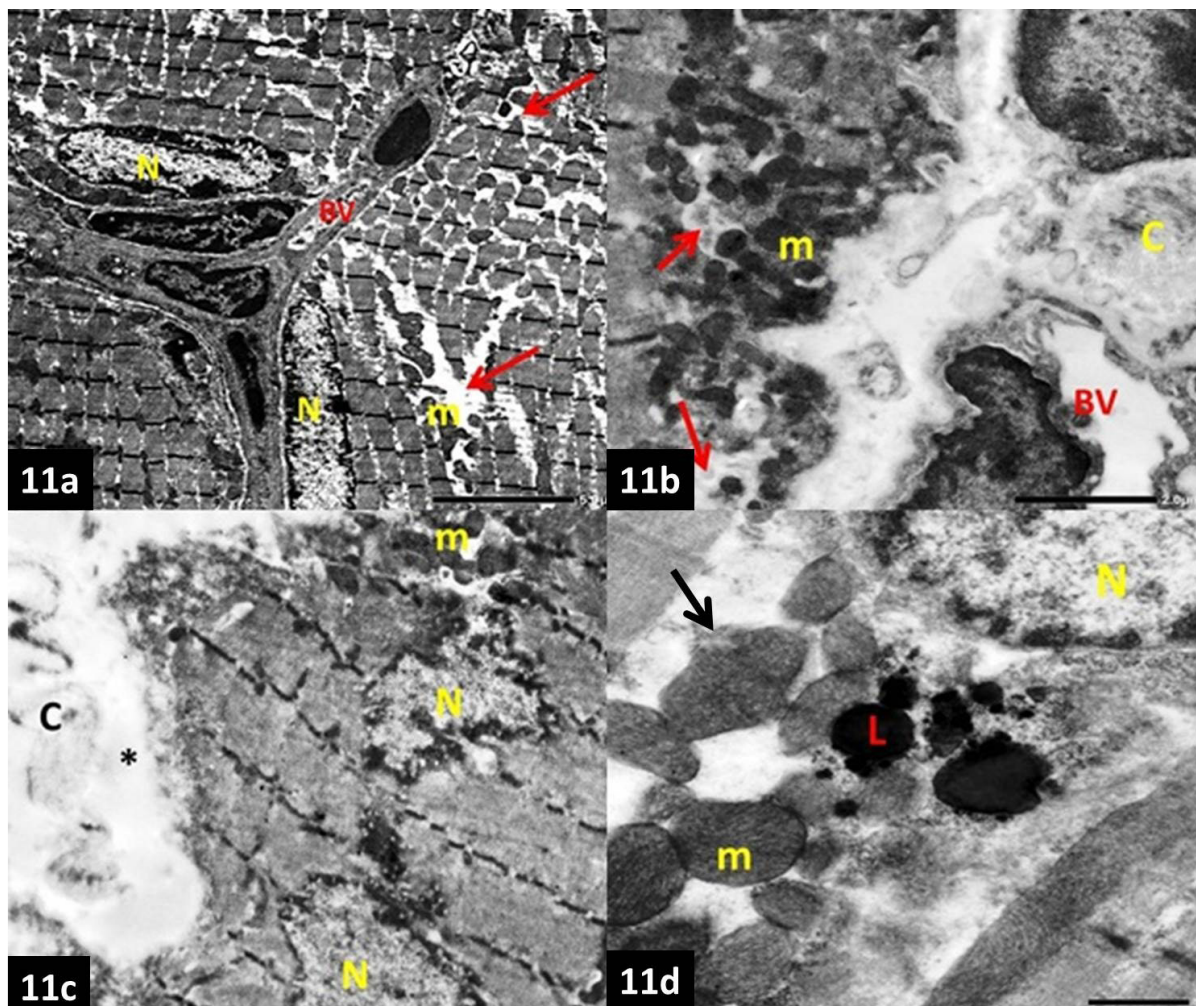
Figs. 11a- d: Electron micrographs of a gastrocnemius muscle of subgroup IIA (untreated group): 11a&11b- focal patches of myofibrillar loss (red arrows) occupied by mitochondria (m). N; sub-sarcolemmal nucleus in a. Notice some collagen fibers (C) and irregular blood vessel (BV) in b. 11c- An injured muscle fiber with interrupted myofibrils and overcrowded deeply situated irregular euchromatic nuclei (N). Numerous aggregated mitochondria (m) are also seen. Notice: collagen fibers (C) and colloid-like material (*). 11d- Numerous mitochondria (m) at the perinuclear region, some of which show disrupted cristae and rupture of its membranes (arrow). L; lysosome. Mic. Mag. 11a) X1500, 11b) X2000, 11c) X3000, 11d) X10000
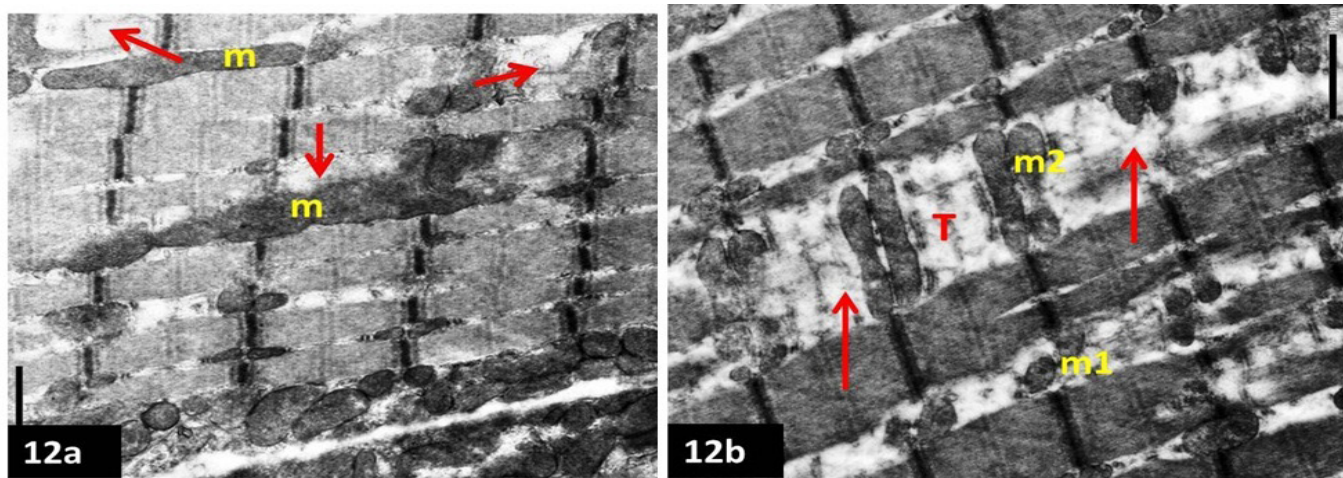
Figs. 12a, b: Electron micrographs of a gastrocnemius muscle of the same subgroup showing focal areas of myofibrillar loss (arrows). 12a- longitudinally oriented mitochondria are seen in between the myofibrils, some are giant and fused together (m). 12b- Many longitudinally oriented mitochondria (m1) of different sizes and shapes are seen in between the myofibrils, others are transversely oriented in register with Z lines at the damaged areas (m2) and few show disrupted cristae. Note: prominent T-tubules (T) at the site of myofibrillar loss. Mic. Mag. X6000
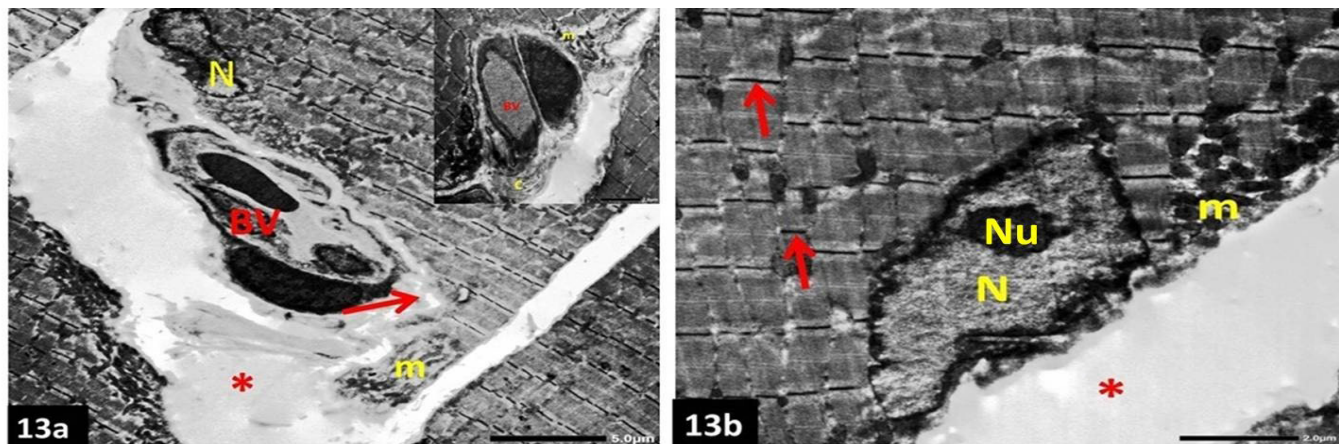
Figs. 13a, b: Electron micrographs of a gastrocnemius muscle of subgroup IIB (PRP subgroup): 13a- injured muscle fibers (arrow) with interrupted myofibrils and numerous pleomorphic mitochondria (m) at their edges. Notice the presence of wide area of colloid-like material (*). BV; blood vessel, N; irregular subsarcolemmal nucleus. Inset: collagen fibers deposition (C) at the site of injury. 13b- sub-sarcolemmal euchromatic irregular nucleus (N) among disarrayed myofibrils (arrows). Sub-sarcolemmal accumulation of moderate number of mitochondria (m) is also noticed. Notice colloidal like material (*). Nu; nucleolus. Mic. Mag. 13a) X1500, inset & 13b) X3000
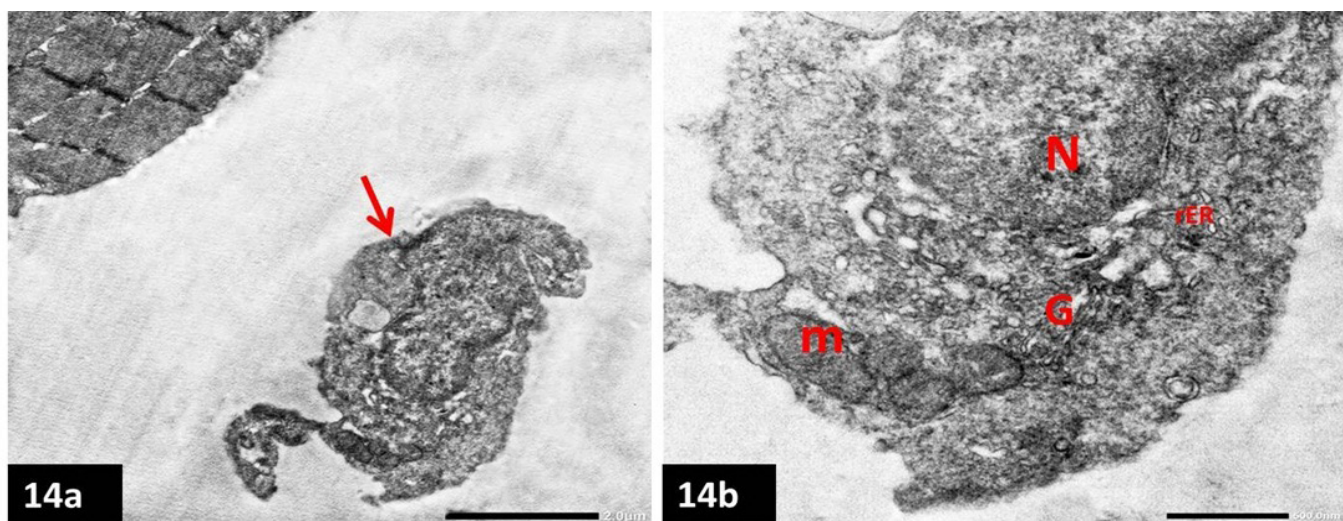
Figs. 14 a, b: Electron micrographs of a gastrocnemius muscle of the same subgroup showing: 14a- An ovoid migratory cell (arrow) in the vicinity of a part of the striated muscle fiber. 14b- At a higher magnification this cell has an euchromatic nucleus (N) with several cell organelles including mitochondria (m), rough endoplasmic reticulum (rER) and Golgi apparatus (G). Mic. Mag. 14a) X4000, 14b) X12000
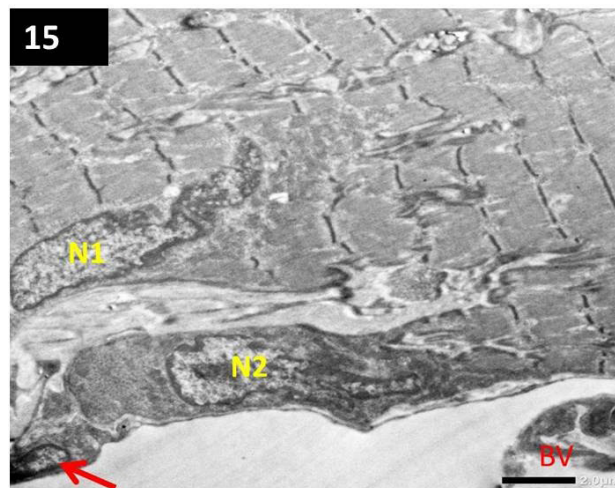
Fig. 15: An electron photomicrograph of a gastrocnemius muscle of the subgroup IIB, showing an irregularly striated muscle fiber with a deeply situated irregular euchromatic nucleus (N1). Some migratory cells are seen along the border of this myofiber, one has a flattened nucleus (N2), another small elongated cell has more flattened nucleus and a cytoplasmic process bordering the neighboring cell (arrow). BV, blood vessel. Mic. Mag. X2000
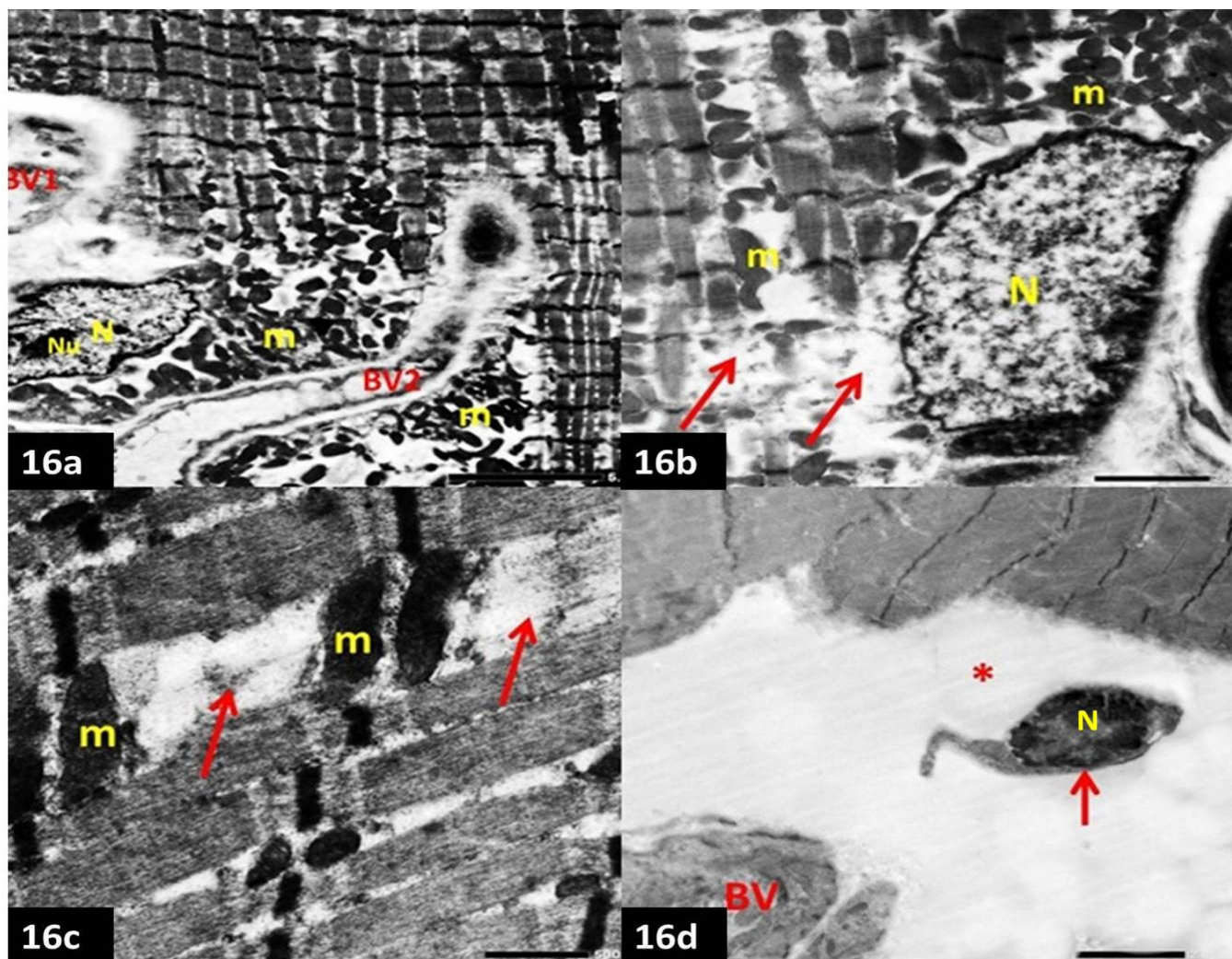
Figs. 16a-d: Electron micrographs of a gastrocnemius muscle of subgroup IIC (Losartan subgroup), showing: 16a- An injured and interrupted muscle fiber with wide areas of myofibrillar loss. Blood vessels are seen growing towards the injured area (BV1, BV2). (BV2) is surrounded by numerous irregularly arranged mitochondria (m) of variable sizes. Notice the euchromatic irregular nucleus (N) with prominent nucleolus (Nu). 16b- Multiple areas of myofibrillar loss (arrows) surrounded by numerous irregularly arranged pleomorphic mitochondria (m). An irregular subsarcolemmal euchromatic nucleus (N) is also noticed. 16c- Areas of myofibrillar loss (arrows) occupied by transversely oriented mitochondria (m). Notice loss of the regular striations of the muscle fiber. 16d- Small ovoid migratory cell (arrow) with a large heterochromatic nucleus (N) adjacent to injured muscle fiber. Notice the colloid-like material in the interstitial space (*).BV; Blood vessel. Mic. Mag. 16a) X1500, 16b& 16d) X3000, 16c) X10000
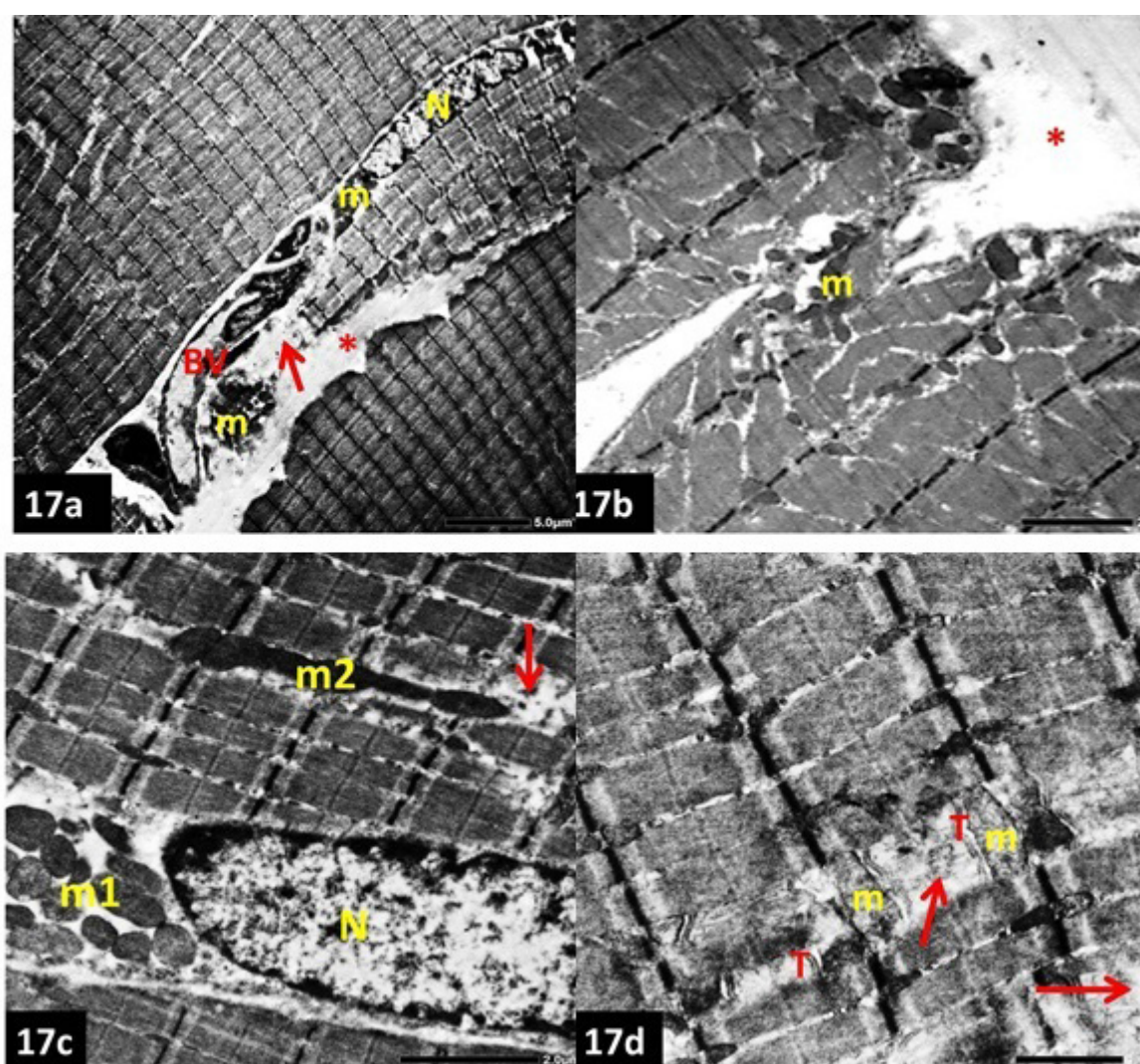
Figs. 17a-d: Electron micrographs of a gastrocnemius muscle of subgroup IID (PRP+losartan subgroup), showing: 17a- An injured and interrupted muscle fiber with an area of myofibrillar loss (arrow) occupied by migratory blood vessel (BV) among proliferated numerous mitochondria (m). Notice well registered striated myofibrils and colloid-like material (*). N; nucleus. 17b- An injured myofiber with an irregular outline and a retrieval of its continuity associated with irregularly arranged pleomorphic mitochondria (m). Notice: the colloid-like material (*). 17c- A sub-sarcolemmal euchromatic nucleus (N) and multiple mitochondria (m1) at the nuclear pole. Focal areas of myofibrillar loss (arrow) surrounded by giant matted mitochondria (m2) are also seen. 17d- A striated muscle fiber with limited areas of myofibrillar loss (arrows). Notice: the transversely oriented mitochondria (m) and associated evident T-tubules (T). Mic. Mag. 17a) X1000, 17b) X3000, 17c) X4000, 17d) X6000

DISCUSSION

Muscle contusions are the most prevalent type of muscle injury, accounting for the vast majority of sports-related injuries. So, the need for new strategies to restore or speed up the process of muscle tissue regeneration represents an enormous challenge to researchers[2]. Thus, in the current work, the modulating effect of PRP or losartan as well as the combined treatment was studied on the healing of skeletal muscle after a contusion injury in a gastrocnemius muscle of a rat model.

In the present study, the histological findings of subgroup IIA, which received no treatment, were indicative of commencement of degenerative changes[22]. They were in agreement with other researchers who reported the necrosis of the muscle fibers, which was initiated by a breakdown of local homeostasis, specifically an uncontrolled inflow of calcium through sarcolemma lesions. Excess sarcoplasmic

calcium induces the activation of proteases and hydrolases, which adds to muscle damage, as well as enzymes that stimulate the production of mitogenic chemicals for muscle and immune cells[23,24]. In addition, an increase in physical pressure and temporary ischemia followed by rapid physical recovery lead to intercellular edema in the form of exudate or colloid like material leading to widening of the interstitial spaces in between the muscle fibers which was detected in the current work[25].

In this study, subgroup IIA showed few fibers exhibited subsarcolemmal or deeply situated large lightly stained irregular nuclei. Different degrees of cellular proliferation with pale stained nuclei; most probably the myoblasts; were seen migrating towards the injured fibers, which became massive in some areas forming a multinucleated syncytium. The perivascular areas revealed increased cellularity with some cells with flattened nuclei, while others were with

pale stained ovoid nuclei. These morphological changes suggested that modest regenerative processes had begun as proved by Järvinen *et al*.[26] and were confirmed in the current work by the immunohistochemical results which exhibited positive CD34 cells surrounding the blood vessels, in the endomysium, within the proliferating cells and along the lateral boundaries of some fibers.

On the other hand, the current interstitial hemorrhage and the congestion of the blood vessels which were associated with extravasation of blood in-between the injured muscle fibers, were previously encountered by other investigators[27,28]. These were attributed to tissue hypoxia, which induces an increase in the capillary permeability.

In the current work, the histological findings were further supported by the electron microscopic examination. One of the explanations of mitochondrial changes is that they are the major sensitive cell organelles that can be deleteriously affected. Some mitochondria showed disrupted cristae and irregular outline which may be due to the production of oxygen free radicals at the site of injury. Reports have suggested that this is an adaptive process at a subcellular level to unfavorable environments[29]. Mitochondria aim to reduce intracellular reactive oxygen species (ROS) levels by reducing oxygen consumption, and if they are successful, these mitochondria return to their normal shape and function. In addition, many fibers revealed irregular arrangement and orientation of the mitochondria which could be contributed to mitochondrial transport failure due to cytoskeletal protein disruption (actin, tubulin, or motor proteins such as kinesin)[30,31].

On the other hand, some fibers revealed accumulation of lysosomes which was also stated by Musarò[32] who demonstrated lysosomal vesicles inserted at the site of the disrupted sarcolemma. Lysosomes perform an important part in the resealing of the plasma membrane and removing any residual necrotic material. In addition, the cells most impacted by the injury also experienced distension of the sarcotubular system responsible for the execution of intracellular membrane polarization and revealed prominent triads at the site of myofibrillar loss. This finding was also mentioned in other studies, which showed that T-tubule system structural alterations are significantly linked to myofibrillar disturbance[33,34].

Excessive collagen fiber deposition was also noticed in the present work by light and electron microscopic examinations of subgroup IIA and was confirmed by morphometric measurements. This was also reported by Petrilli *et al*[35]. By secreting extracellular matrix proteins such as collagen types I and III, fibronectin, elastin, proteoglycans, laminin and numerous growth factors, fibroblasts play a crucial role in muscle tissue repair[36]. In such cases, the scar can create a mechanical barrier against the diffusion of nutrients and the migration of new blood vessels to the myofibers. It also can prevent the migration and fusion of the new muscle cells. This can change the mechanical properties of the muscle (such as elasticity and strength), resulting in fibrosis and incomplete muscle healing[37].

In the current study, muscle specimens obtained from PRP-treated subgroup revealed regenerative signs. The light microscopic features in this subgroup included injured and interrupted muscle fibers with pale eosinophilic sarcoplasm. Evident hypercellularity was in the form of cells with pale stained ovoid nuclei, others with flattened nuclei and adipocytes. Moreover, cellular migration with attempt of myotube formation was depicted. This was further confirmed by ultrastructural findings, included multiple sub-sarcolemmal or deeply situated euchromatic nuclei with irregular outline. In addition, numerous mitochondria were depicted either at the site of myofibrillar loss or along the muscle fibers. Migratory cells with different sizes and irregular nuclei, occasionally associated with blood vessels were also noticed. Some myofibers were bordered by flattened cells with flat nuclei.

The idea behind PRP is that the additional growth factors released by the platelets will help to speed up the natural healing process[38]. This was in agreement with other studies[39,40], which indicated that upon the injection of PRP in the muscle lesion, the local development of the platelet-rich fibrin scaffold affords hemostasis and allows for delay delivery of cytokines and growth factors from platelets and plasma such as VEGF, FGF, PDGF, TNF-α, IGF-1, IGF-2, TGF-β1, FGFs, HGF, IL-6 and HGF[40,41]. This molecular pool influences the different stages of regeneration outlined as apoptosis/necrosis, innate immune response, angiogenesis, cell proliferation and differentiation. It has been reported that it can alter fibroblast migration, myoblast proliferation and enhance angiogenesis[4,7].

The cells which revealed pale stained ovoid nuclei are most probably satellite cells. The studies of damage-induced activation of satellite cells showed that the injury results in the emission of growth factors from the muscles themselves which may allow them to act as "wound hormones" very instantly to activate satellite cells and initiate their migration to the site of muscle regeneration and repair, where they would be differentiated into myoblasts[42,43]. The myoblasts, within their column form an elongated multinucleated syncytium; this was detected in the current work, along the altered sarcolemmal tubes where rows of nuclei are found. This is confirmed by immunohistochemical staining with anti C34. The positive cells in subgroup IIB also appeared inside the muscle fibers in addition to the reaction around the blood vessels and in the connective tissue in between the muscle fibers indicating the migration of the s9atellite cells and subsequently advanced muscle regeneration[44].

Moreover, the current study revealed adipocytes at the injury site and it was also shown in other studies[45]. Single cells from the satellite-cell compartment have been shown to have the ability to produce myogenic, fibroblastic, and adipogenic colonies in *vitro*

On the other hand, the cells noticed with flattened nuclei could be interpreted as fibroblasts which were also described in previous studies (46). PRP has been shown to motivate the proliferation of fibroblasts and enhanced collagen synthesis to fill the gap and anchor the muscle fiber stumps together[46].

The regeneration of the muscle fibers does not progress past the newly formed thin myotube stage unless the needed supply of oxygen for aerobic metabolism has been secured by sufficient capillary ingrowth. Therefore, for multinucleated myofibers, aerobic metabolism is the most important source of energy,[47] and that is why numerous mitochondria were depicted either at the site of myofibrillar loss or along the muscle fiber in the present work.

It has been postulated that PRP could induce muscle fibrosis because of the high concentration of TGF- β1 stored in platelets' α-granules. TGF-β1 is a key factor in the progression of fibrosis in the kidneys, liver, lungs, and the skeletal muscles which stimulates type 1 collagen synthesis and development of fibrosis[47]. However, an excessive deposition of collagen type 1 predisposes the muscle to reinjury and limits its functional recovery[48]. This finding was also confirmed in the current work by the examination of the trichrome-stained slides which showed an excessive deposition of collagen fibers in between the injured fibers, in the endomysium, the perimysium and in the perivascular area.

In losartan subgroup, the examination of the gastrocnemius muscle sections revealed more regenerative signs with decreased fibrosis as compared to the non-treated group. Despite some muscle fibers appeared injured and interrupted, others revealed splitting and branching with deeply situated lightly stained nuclei. Prominent regular cellular migration towards the defected sites was noticed forming multinucleated syncytium and associated with neovascularization in other areas.

Tawfik *et al*[11] have reported that the restoration of vascular supply to the injured area is another crucial hallmark of muscle regeneration, which is required for the following morphological and functional recovery of the injured muscle fibers. In addition, it has an effect on the distribution of recruited inflammatory cells and regeneration-related factors (growth factors, cytokines, chemokines), as well as at the paracrine effect between satellite and endothelial cells that affects the regenerative process. Angiogenesis occurs as a result of the autocrine release of angiogenic factors such as fibroblast growth factor (FGF) by macrophages and endothelial cells[49].

In addition, limited collagen fibers at the large defective areas were also revealed in subgroup IIC with less detected cells with flattened nuclei. These findings were correlated with trichrome-stained sections and morphometric measurements that showed significantly lowered collagen fibers deposition than the untreated subgroup.

It has been reported that direct application of antifibrotic agents as losartan inhibits the scar formation in the injured muscles. Such agents are specific inhibitors of TGF-β1; a growth factor that is thought to be involved in the development of scar tissue during skeletal muscle healing[50,51]. However, the timing of administration of losartan in the current work was on day 3 post-injury and this was also chosen by other investigators[52,53]. This was attributed to that during the healing process, the mRNA expression of TGF-β1 peaks two to three days following muscle injury[54]. Immediate administration, on the other hand, causes abnormal regeneration, which is most likely due to the disruption of the initial inflammatory response and the expected healing process of skeletal muscle[54].

The electron microscopic results of subgroup IIC revealed ovoid migratory cells towards some injured areas which were confirmed by immunohistochemical studies that showed positive reaction around new lightly stained nuclei inside muscle fibers and along its sarcolemma. This in turn supports the hypothesis that in adults, muscle satellite cells are the primary source of myogenic cells, while vessel-related progenitor cells are a secondary source of myogenesis and can also contribute to neoangiogenesis in the human muscle[55].

The histological findings of subgroup IID (which received both the PRP and losartan) revealed evident regenerating fibers with minimal structural changes. Most of the skeletal muscle fibers appeared with multiple deeply situated and sub-sarcolemmal lightly stained nuclei aligned along the longitudinal axis forming myotubes. Many multinucleated syncytia, branched fibers and cross bridging of some fibers were also depicted. Migrating blood vessels with perivascular hypercellularity and few connective tissue fibers were commonly encountered.

Myotube formation, which was detected in the present work, is considered as an important sign which occurs during the later phases of muscle regeneration[56]. Muscle nuclei begin to align along the muscle fiber's longitudinal axis, becoming central in position, which is a feature of myotube development or muscle fibers undergoing healing. The central nuclei migrate to the surface of the muscle fiber and increase in size upon the completion of terminal differentiation[32].

While attempting to pierce through the scar that separates them, the myofibers of the surviving muscle stumps create many branches[57]. However, after only a little distance of extension, the tips of the branches begin to adhere to the connective tissue at their ends. These myofibers are still small, and their nuclei are located near the center. These results were also described by other researchers who mentioned that these fundamental morphological characteristics are newly formed myofibers with centrally located myonuclei and small caliber[58]. These findings went hand in hand with the electron microscopic results of subgroup IID as most of the muscle fibers showed normal ultrastructural features except for

few scattered areas of injured and interrupted myofibrils with retrieval of its continuity. Nearly all muscle fibers were well registered with sub-sarcolemmal euchromatic nuclei. Migratory blood vessels were also noticed at the site of injury of some fibers.

Moreover, limited collagen fibers deposition even in the large defective areas was noticed and supported by the trichrome-stained slides which detected almost the control pattern of collagen distribution in some areas. Blocking TGF- β1 by losartan inhibits the formation of fibrosis in injured muscle and PRP would speed up the muscle's functional recovery[52]. This was also noted in a study carried out by Tsai *et al*.[59] who found that the fibrotic areas in the group received mixed therapies (PRP and Suramin) were significantly less prevalent than the other experimental groups.

The examination of immune stained slides of subgroup IID, revealed less areas housed by CD34 positive cells. It may be linked to a more thorough restoration of histological structure where the fibers were relatively organized[60].

Finally, the current study was able to demonstrate greater improvements in the muscle healing in the PRP, losartan and PRP +losartan subgroups compared by the untreated group three weeks after inducing the injury. However, the PRP+losartan subgroup showed significantly better histological results compared to all other subgroups in the form of muscle regeneration and reduced the development of fibrosis.

CONCLUSION

The combined PRP + losartan treatment regimen, which are both currently clinically available, has the potential to speed up the recovery of skeletal muscle following a muscle contusion.

CONFLICT OF INTERESTS

There are no conflicts of interest.

REFERENCES

1. Cianforlini M, Grassi M, Coppa V, Manzotti S, Orlando F, Mattioli-Belmonte M, *et al*. Skeletal muscle repair in a rat muscle injury model: the role of growth hormone (GH) injection. Eur Rev Med Pharmacol Sci 2020; 24(16):8566-8572.

2. Paun B, Leon DG, Cabello AC, Pages RM, de la Calle Vargas E, Muñoz PC, *et al*. Modelling the skeletal muscle injury recovery using in *vivo* contrast-enhanced micro-CT: a proof-of-concept study in a rat model. Eur Radiol Exp 2020; 4(1):33.

3. Marmolejo-Martínez-Artesero S, Romeo-Guitart D, Venegas V, Marotta M, Casas C. NeuroHeal Improves Muscle Regeneration after Injury. Cells 2020; 10(1):22.

4. Fang J, Wang X, Jiang W, Zhu Y, Hu Y, Zhao Y, *et al*. Platelet-Rich Plasma Therapy in the Treatment of Diseases Associated with Orthopedic Injuries. Tissue Eng Part B Rev 2020; 26(6):571-585.

5. Xu J, Gou L, Zhang P, Li H, Qiu S. Platelet-rich plasma and regenerative dentistry. Aust Dent J 2020; 65(2):131-142.

6. Everts P, Onishi K, Jayaram P, Lana JF, Mautner K. Platelet-Rich Plasma: New Performance Understandings and Therapeutic Considerations in 2020. Int J Mol Sci 2020; 21(20):7794.

7. El-Mahalaway AM , El-Azab NE. Impacts of resveratrol versus platelet-rich plasma for treatment of experimentally lithium-induced thyroid follicular cell toxicity in rats. A histological and immunohistochemical study. Ultrastruct Pathol 2019;43;(1):80-93.

8. Tischer T, Bode G, Buhs M, Marquass B, Nehrer S, Vogt S, *et al*. Platelet-rich plasma (PRP) as therapy for cartilage, tendon and muscle damage - German working group position statement. J Exp Orthop 2020; 7(1):64.

9. Ismaeel A, Kim JS, Kirk JS, Smith RS, Bohannon WT, Koutakis P. Role of Transforming Growth Factor-β in Skeletal Muscle Fibrosis: A Review. Int J Mol Sci 2019; 20(10):2446.

10. Kim J, Lee J. Role of transforming growth factor-β in muscle damage and regeneration: focused on eccentric muscle contraction. J Exerc Rehabil 2017; 13(6):621-626.

11. Tawfik VL, Quarta M, Paine P, Forman TE, Pajarinen J, Takemura Y, *et al*. Angiotensin receptor blockade mimics the effect of exercise on recovery after orthopaedic trauma by decreasing pain and improving muscle regeneration. J Physiol 2020; 598(2):317-329.

12. Kalynovska N, Diallo M, Sotakova-Kasparova D, Palecek J. Losartan attenuates neuroinflammation and neuropathic pain in paclitaxel-induced peripheral neuropathy. J Cell Mol Med 2020; 24(14):7949-7958.

13. Hadipour-Lakmehsari S, Al Mouaswas S. Reduction of pain and improved muscle biology with the administration of losartan and delayed exercise in a murine trauma model. J Physiol 2020; 598(4):631-632.

14. Huard J, Bolia I, Briggs K, Utsunomiya H, Lowe WR, Philippon MJ. Potential Usefulness of Losartan as an Antifibrotic Agent and Adjunct to Platelet-Rich Plasma Therapy to Improve Muscle Healing and Cartilage Repair and Prevent Adhesion Formation. Orthopedics 2018; 41(5):e591-e597.

15. Delos D, Leineweber MJ, Chaudhury S, Alzoobaee S, Gao Y, Rodeo SA. The effect of platelet-rich plasma on muscle contusion healing in a rat model. Am J Sports Med 2014; 42(9):2067-2074.

16. Fukushima K, Badlani N, Usas A, Riano F, Fu FH, Huard J. The use of an antifibrosis agent to improve muscle recovery after laceration. Am J Sports Med 2001; 29(4):394-402.

17. Quarteiro ML, Tognini JRF, de Oliveira ELF, Silveira I. The effect of platelet-rich plasma on the repair of muscle injuries in rats. Rev Bras Ortop 2015; 50(5):586-595.

18. Carleton HM, Drury RAB, Wallington EA. Carleton's histological technique. USA: Oxford University Press 1980.

19. Suvarna KS, Layton C, Bancroft JD. Bancroft's theory and practice of histological techniques. Amsterdam, Netherlands: Elsevier Health Sciences; 2018.

20. Pusztaszeri MP, Seelentag W, Bosman FT. Immunohistochemical expression of endothelial markers CD31, CD34, von Willebrand factor, and Fli-1 in normal human tissues. J Histochem Cytochem 2006; 54(4):385-395.

21. Glauert AM, Lewis PR. Biological specimen preparation for transmission electron microscopy. USA: Princeton University Press; 2014.

22. MakovickÃ P, MakovickÃ P. Histological aspects of skeletal muscle fibers splitting of C57BL/6NCrl mice. Physiological Research 2020;69(2):291-296.

23. Mázala DA, Pratt SJ, Chen D, Molkentin JD, Lovering RM, Chin ER. SERCA1 overexpression minimizes skeletal muscle damage in dystrophic mouse models. Am J Physiol Cell Physiol 2015; 308(9):C699-709.

24. Tidball JG. Mechanisms of muscle injury, repair, and regeneration. Compr Physiol 2011; 1(4):2029-2062.

25. Kuroda Y, Togashi H, Uchida T, Haga K, Yamashita A, Sadahiro M *et al*. Oxidative stress evaluation of skeletal muscle in ischemia–reperfusion injury using enhanced magnetic resonance imaging. Sci Rep 2020;10:10863.

26. Järvinen TA, Järvinen TL, Kääriäinen M, Äärimaa V, Vaittinen S, Kalimo H, *et al*. Muscle injuries: optimising recovery. Best Pract Res Clin Rheumatol 2007; 21(2):317-331.

27. Valle-Tenney R, Rebolledo D, Acuña MJ, Brandan E. HIF-hypoxia signaling in skeletal muscle physiology and fibrosis. J Cell Commun Signal. 2020;14(2):147-158.

28. Drouin G, Couture V, Lauzon MA, Balg F, Faucheux N, Grenier G. Muscle injury-induced hypoxia alters the proliferation and differentiation potentials of muscle resident stromal cells. Skelet Muscle 2019;9(1):18.

29. Romanello V, Sandri M. The connection between the dynamic remodeling of the mitochondrial network and the regulation of muscle mass. Cell Mol Life Sci 2021;78(4):1305-1328.

30. Otera H, Ishihara N, Mihara K. New insights into the function and regulation of mitochondrial fission. Biochim Biophys Acta Mol Cell Res 2013; 1833(5):1256-1268.

31. Elgass K, Pakay J, Ryan MT, Palmer CS. Recent advances into the understanding of mitochondrial fission. Biochim Biophys Acta Mol Cell Res 2013; 1833(1):150-161.

32. Musarò A. Muscle Homeostasis and Regeneration: From Molecular Mechanisms to Therapeutic Opportunities. Cells 2020; 9(9):2033.

33. Lauritzen F, Paulsen G, Raastad T, Bergersen LH, Owe SG. Gross ultrastructural changes and necrotic fiber segments in elbow flexor muscles after maximal voluntary eccentric action in humans. J Appl Physiol 2009; 107(6):1923-1934.

34. Stožer A, Vodopivc P, KRIŽANČIĆ BOMBEK L. Pathophysiology of Exercise-Induced Muscle Damage and Its Structural, Functional, Metabolic, and Clinical Consequences. Physiol. Res 2020 ;69(4):565-598.

35. Petrilli LL, Spada F, Palma A, Reggio A, Rosina M, Gargioli C ,*et al*. High-Dimensional Single-Cell Quantitative Profiling of Skeletal Muscle Cell Population Dynamics during Regeneration. Cells 2020; 9(7):1723.

36. Bersini S, Gilardi M, Mora M, Krol S, Arrigoni C, Candrian C, *et al*. Tackling muscle fibrosis: From molecular mechanisms to next generation engineered models to predict drug delivery. Adv Drug Deliv Rev 2018; 129:64-77.

37. Martins-Bach AB, Bachasson D, Araujo E, Soustelle L, de Sousa P, Fromes Y, *et al*. Non-invasive assessment of skeletal muscle fibrosis in mice using nuclear magnetic resonance imaging and ultrasound shear wave elastography. Sci Rep 2021; 11: 284.

38. Setayesh K, Villarreal A, Gottschalk A, Tokish JM, Choate WS. Treatment of Muscle Injuries with Platelet-Rich Plasma: a Review of the Literature. Curr Rev Musculoskelet Med 2018;11(4):635-642.

39. Hillege MMG, Galli Caro RA, Offringa C, de Wit GMJ, Jaspers RT, Hoogaars WMH. TGF-β Regulates Collagen Type I Expression in Myoblasts and Myotubes via Transient Ctgf and Fgf-2 Expression. Cells 2020; 9(2):375.

40. Forcina L, Cosentino M, Musarò A. Mechanisms Regulating Muscle Regeneration: Insights into the Interrelated and Time-Dependent Phases of Tissue Healing. Cells 2020; 9(5):1297.

41. Malanga GA, Goldin M. PRP: review of the current evidence for musculoskeletal conditions. Curr Phys Med Rehabil Rep 2014; 2(1):1-15.

42. Moriscot A, Miyabara EH, Langeani B, Belli A, Egginton S, Bowen TS. Firearms-related skeletal muscle trauma: pathophysiology and novel approaches for regeneration. NPJ Regen Med 2021;6(1):17.

43. Kaczmarek A, Kaczmarek M, Ciałowicz M, Clemente FM, Wolański P, Badicu G, *et al*. The Role of Satellite Cells in Skeletal Muscle Regeneration-The Effect of Exercise and Age. Biology (Basel) 2021;10(10):1056.

44. Kunze KN, Hannon CP, Fialkoff JD, Frank RM, Cole BJ. Platelet-rich plasma for muscle injuries: A systematic review of the basic science literature. World J Orthop 2019;10(7):278-291.

45. Theret M, Rossi FMV, Contreras O. Evolving Roles of Muscle-Resident Fibro-Adipogenic Progenitors in Health, Regeneration, Neuromuscular Disorders, and Aging. Front Physiol 2021;12:673404.

46. Molina T, Fabre P, Dumont NA. Fibro-adipogenic progenitorsinskeletalmusclehomeostasis,regeneration and diseases. Open Biol 2021;11(12):210110.

47. Garg K, Corona BT, Walters TJ. Therapeutic strategies for preventing skeletal muscle fibrosis after injury. Front Pharmacol 2015; 6:87.

48. Van Meeteren LA, Ten Dijke P. Regulation of endothelial cell plasticity by TGF-β. Cell Tissue Res 2012; 347(1):177-186.

49. Gardner T, Kenter K, Li Y. Fibrosis following acute skeletal muscle Injury: mitigation and reversal potential in the clinic. Journal of Sports Medicine 2020 ; 2020.

50. Garg K, Corona BT, Walters TJ. Losartan administration reduces fibrosis but hinders functional recovery after volumetric muscle loss injury. J Appl Physiol 2014; 117(10):1120-1131.

51. Chan YS, Li Y, Foster W, Horaguchi T, Somogyi G, Fu FH, *et al*. Antifibrotic effects of suramin in injured skeletal muscle after laceration. J Appl Physiol 2003; 95(2):771-780.

52. Terada S, Ota S, Kobayashi M, Kobayashi T, Mifune Y, Takayama K, *et al*. Use of an antifibrotic agent improves the effect of platelet-rich plasma on muscle healing after injury. JBJS 2013; 95(11):980-988.

53. Laumonier T, Menetrey J. Muscle injuries and strategies for improving their repair. J Exp Orthop 2016; 3(1):15.

54. Obayashi T, Uehara K, Ota S, Tobita K, Ambrosio F, Cummins JH, *et al*. The timing of administration of a clinically relevant dose of losartan influences the healing process after contusion induced muscle injury. J Appl Physiol 2012; 114(2):262-273.

55. Sicherer ST, Venkatarama RS, Grasman JM. Recent Trends in Injury Models to Study Skeletal Muscle Regeneration and Repair. Bioengineering 2020; 7(3):76.

56. Anderson JE. Key concepts in muscle regeneration: muscle "cellular ecology" integrates a gestalt of cellular cross-talk, motility, and activity to remodel structure and restore function. Eur J Appl Physiol 2021; 20:1–28.

57. Järvinen TA, Järvinen M, Kalimo H. Regeneration of injured skeletal muscle after the injury. Muscles Ligaments Tendons J 2013; 3(4):337.

58. Kelc R, Trapecar M, Gradisnik L, Rupnik MS, Vogrin M. Platelet-rich plasma, especially when combined with a TGF-beta inhibitor promotes proliferation, viability and myogenic differentiation of myoblasts in *vitro*. PLoS One 2015;10(2):e0117302.

59. Tsai WC, Yu TY, Chang GJ, Lin LP, Lin MS, Pang JH. Use of Platelet-Rich Plasma Plus Suramin, an Antifibrotic Agent, to Improve Muscle Healing After Injuries. Am J Sports Med 2021; 49(11):3102-3112.

60. Zickri MB, El Aziz DHA. Relation between microcurrent therapy and satellite cells in the regeneration of induced skeletal muscle injury in rat. Egypt J Histol 2013; 36(2):409-417.

الملخص العربى

التأثير التآزري المحتمل للبلازما الغنية بالصفائح الدموية واللوسارتان على إصابة العضلة الهيكلية المستحدثة تجريبياً في ذكور الجرذان البيضاء البالغة: دراسة هيستولوجية و هيستوكيميائية مناعية

أميرة هاشم محمد نعينع، مشيره علي رضا الهنيدي، هدي محمود أحمد خليفة، سيلفيا كميل صديق ساويرس

قسم الهستولوجيا ـ كلية الطب ـ جامعة الإسكندرية

المقدمة: لا يزال التقليل من الإعاقة بعد إصابات العضلات الهيكلية يمثل تحديًا، وقد أدى فهم مساهمة عوامل النمو إلى ظهور اهتمام كبير باستخدام البلازما الغنية بالصفائح الدموية. خط آخر في العلاج هو استخدام مضادات التليف مثل اللوسارتان.

الهدف: هو اختبار التأثير العلاجي للبلازما الغنية بالصفائح الدموية واللوسارتان والعلاج المشترك على إصابة العضلات الهيكلية.

طرق البحث: ـ تم تقسيم اثنين و أربعين من ذكور الجرذان البيضاء البالغة إلى مجموعتين: المجموعة الأولى (مجموعة ضابطة) والمجموعة الثانية (مجموعة الجرذان المصابة) والتي تم تقسيمها إلى ٤ مجموعات فرعية متساوية : مجموعة لم تتلقى علاج ، مجموعة تلقت حقنة عضلية واحدة ١٠٠ ميكرولترمن البلازما الغنية بالصفائح الدموية ،مجموعة تلقت جرعة واحدة من ١٠ مجم / كجم من وزن الجسم / يوم لوسارتان عن طريق الفم، مجموعة تلقت العلاج المشترك. تم ذبح الجرذان بعد ثلاثة أسابيع من احداث الأصابة واعداد عضلة الساق gastrocnemius للفحص المجهري الضوئى والإلكترونى النافذ، بالإضافة إلى إجراء دراسة هستوكيميائية مناعية لخلايا CD٣٤ الأيجابية.

النتائج: أظهرت مجموعة IIA الياف عضلية متقطعة مع فقد الليبفات ، بينما كشفت المجموعتان IIB و IIC عن المزيد من التغييرات التجددية . كما تم الكشف عن زيادة خلوية مهاجرة واضحة و لوحظ نمو اوعية دموية جديدة في مناطق أخرى من المجموعة IIC، أما المجموعة IID فقد أظهرت أليافًا متجددة في مراحل مختلفة مع تغييرات هيكلية قليلة، كما أظهرت النتائج تفاعلًا إيجابيًا للصبغة الهستوكيميائية المناعية ضد CD٣٤ على طول حدود بعض ألياف العضلات في المجموعة IIA ، بينما امتد التفاعل الإيجابي في المجموعات IIB و IIC و IID إلى الحدود الجانبية وداخل بعض الألياف المصابة وحول الأنوية الباهتة الجديدة ، مما يعبر عن تجديد العضلات.

الخلاصة: العلاج المشترك للبلازما الغنية بالصفائح الدموية واللوسارتان يمكن أن يحسن من التئام العضلات الهيكلية بشكل عام بعد كدمة العضلات.